Theor Chem Acc (2010) 127:727–733
DOI 10.1007/s00214-010-0784-9

REGULAR ARTICLE

Chemical functionalization of pyridine-like and porphyrin-like nitrogen-doped carbon (CN_x) nanotubes with transition metal (TM) atoms: a theoretical study

Yan Shang · Jing-xiang Zhao · Hong Wu · Qing-hai Cai · Xiao-guang Wang · Xuan-zhang Wang

Received: 30 May 2010 / Accepted: 15 July 2010 / Published online: 31 July 2010

Abstract It is well known that chemical functionalization of carbon nanotubes (CNTs) can offer an effective route to modify their properties, thus significantly widening their application areas. In the present work, through spin-polarized density functional theory (DFT) calculations, we have systemically studied the chemical functionalization of pyridine-like and porphyrin-like nitrogen-doped carbon (CN_x) nanotubes with 13 different transition metals (TMs = Sc, Ti, V, Cr, Mn, Fe, Co, Ni, Cu, Zn, Pt, Pd, and Au). Particular attention is paid to searching for the most stable configurations, calculating the corresponding binding energies, and exploring the effects of the chemical functionalization of TMs on the electronic properties of the two CN_x nanotubes. We find that (1) due to the strong interaction between the d orbitals of TMs and the p orbitals of N atoms, the binding strengths of TMs with the two CN_x nanotubes are significantly enhanced when compared to the pure CNTs; (2) the electronic properties of CN_x nanotubes can be effectively modified in various ways, which are strongly dependent on the adsorbed TMs.

Y. Shang
School of Chemical and Environmental Engineering, Harbin University of Science and Technology, Harbin 150040, People's Republic of China

J. Zhao (✉) · Q. Cai · Xiao-guang Wang · Xuan-zhang Wang
Key Lab for Design and Synthesis of Functionalized Materials and Green Catalysis, School of Chemistry and Chemical Engineering, Harbin Normal University, Harbin 150025, People's Republic of China
e-mail: xjz_hmily@yahoo.com.cn

H. Wu
College of Chemistry and Life Science, Quanzhou Normal University, Fujian 362000, People's Republic of China

Keywords Chemical functionalization · CN_x nanotubes · Transition metal · Density functional theory

1 Introduction

Recently, chemical functionalization of carbon nanotubes (CNTs) with various groups has attracted considerable interest as an efficient way to modify their properties [1–6]. Typically, the electronic and magnetic properties of CNTs can be effectively modified through chemical decoration of transition metals (TMs) [7–9], which greatly expands the potential application areas of CNTs, such as improving the sensitivities of chemical sensors, providing higher reactive sites for gas storages, and developing spintronic devices or catalysts.

On the other hand, the N-doped CNTs, named CN_x nanotubes, have been synthesized in several groups [10–15]. Electron energy loss spectroscopy and X-ray photoelectron spectroscopy measurements indicated the coexistence of pyridine-like and porphyrine-like structures [12, 13]. For the former, nitrogen substitution accompanied with vacancy (labeled as 3NV) is formed in the sidewall of CN_x nanotubes, whose electronic [16], field-emission [17], and electrical transport properties [18] have been systemically investigated. On the contrary, the structure of the latter consists of four nitrogen atoms around a divacancy (labeled as 4ND). Due to the presence of 3NV or 4ND defect, the reactivity of CN_x nanotubes might be greatly enhanced compared with the pure CNT, thus becoming a recently hot topic [15, 19–28]. For example, CN_x nanotubes can be used as gas sensors of toxic species [15, 19]. Moreover, the capability of Li storage in the CN_x tube is significantly increased [20]. Most importantly, the CN_x nanotube is a promising candidate as a support material to

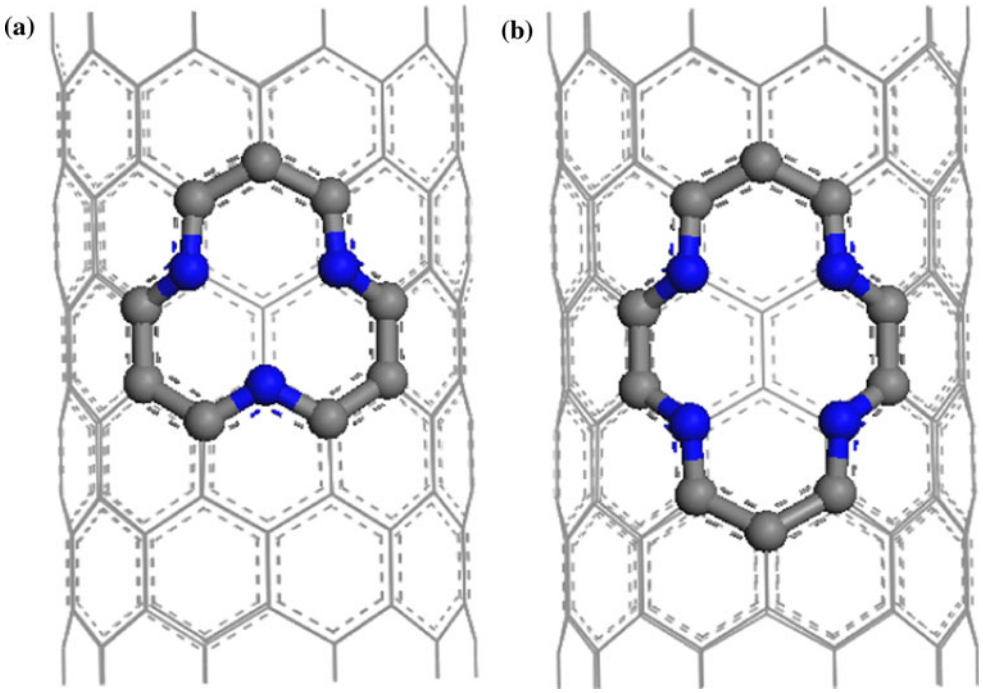

Fig. 1 Optimized structures of the CN_x nanotubes with **a** 3NV and **b** 4ND defects. *Gray* and *blue* balls represent the carbon and nitrogen atoms

immobilize various TM nanoparticles, which have been found to exhibit good catalytic property [24–34]. For example, Yoon et al. [24] have shown that the Pd-decorated CN_x nanotube displays high catalytic activities for Heck, Suzuki, and Songasahira coupling reactions. Furthermore, Shao et al. [25] have demonstrated that the Pt/CN_x nanotube is an excellent material for proton exchange membrane fuel cell. Additionally, Su et al. [26] have shown that the Pt/CN_x nanocatalyst exhibits good catalytic activities toward methanol oxidation and oxygen reduction reactions.

Compared with these experimental advances in the interactions between TMs and CN_x nanotubes, to our knowledge, there are only a few theoretical studies on this issue [35–39]: (1) through density functional theory (DFT) calculations [35, 36], Yang and Li have independently reported that the binding energy of Ni or Pt interacting with the CNT is significantly improved in the presence of the 3NV defect in the CNT. (2) Feng et al. [37] have theoretically studied adsorptions of 12 different TMs on three kinds of CN_x nanotubes, including graphite-like nitrogen (GN), pyridine-like nitrogen (PN), and the vacancy nitrogen (VN) configurations. On aiming to evaluate the catalytic performance of Pt/CN_x nanotube, they have further investigated its interaction with several common species involved in methanol oxidation, including CH_3OH, HCHO, and HCOOH. (3) Titov et al. [38, 40] have explored the stability of Fe-adsorbed CN_x nanotubes with 4ND defect through the bent-cluster model.

However, the following issues still need to be addressed: (1) the effects of various TMs adsorptions on the magnetic and electronic properties of CN_x nanotubes; (2) the bonding nature between different TMs and the CN_x nanotube with 4ND structure. Thus, in the present work, the chemical functionalization of 13 different TMs (Sc, Ti, V, Cr, Mn, Fe, Co, Ni, Cu, Zn, Pd, Pt, and Au) on a (10, 0) CN_x nanotube with 3NV or 4ND defect has been systematically studied through spin-polarized DFT calculations. Particular attention has been paid to locating the most stable adsorption configurations, calculating the corresponding binding energies, and exploring the effects of TMs adsorptions on the properties of the two CN_x nanotubes. Such knowledge might be useful for further studying the adsorptions of TM clusters on CN_x nanotubes.

2 Computational models and methods

In this work, we used the DFT methods, implemented in the $DMOL^3$ package [41, 42], to study the chemical functionalization of 13 different TMs on the two CN_x nanotubes. This method has been widely used in the theoretical calculations of the interaction between the nanotubes and TMs [43–45]. All-electrons calculations were employed with the double numerical plus polarization basis sets (DNP). The exchange correlation energy was described by the Perdew–Burke–Ernzerhof within the generalized-gradient approximation (GGA–PBE) [46]. For the 5d

Table 1 Calculated the TM–C bond lengths, binding energies (E_b) of various TMs adsorbed on the CN_x nanotube with 4ND or 3NV defect, the net magnetic moment of the TM (μ_M) and the TM/CN_x nanotube (μ_{total}), and the charge transferred (C) from TM to the CN_x nanotube

TM	CN_x tube	d_{TM-N}(Å)	E_b (eV)	μ_M/μ_{total} (μ_B)	C(e)
Sc	4ND	2.15[a]	10.94	0.27/1.00	0.65
	3NV	2.01	9.42	0.00/0.00	0.70
Ti	4ND	2.10	10.50	1.34/1.46	0.48
	3NV	1.93	8.72	0.86/0.87	0.57
V	4ND	2.05	7.99	2.46/2.66	0.37
	3NV	1.93	6.43	2.33/2.35	0.43
Cr	4ND	2.03	7.37	3.55/3.83	0.46
	3NV	1.88	5.16	1.95/2.05	0.54
Mn	4ND	1.98	8.13	2.91/3.07	0.29
	3NV	1.85	6.20	0.62/0.65	0.30
Fe	4ND	1.96	9.75	1.91/1.99	0.23
	3NV	1.83	7.87	0.00/0.00	0.29
Co	4ND	1.94	8.52	0.93/0.94	0.18
	3NV	1.87	6.50	1.33/1.50	0.21
Ni	4ND	1.92	8.86	0.00/0.00	0.12
	3NV	1.84	6.66	0.96/1.00	0.17
Cu	4ND	2.01	5.61	0.46/1.00	0.39
	3NV	1.94	4.30	0.00/0.00	0.32
Zn	4ND	2.05	4.44	0.00/0.00	0.47
	3NV	1.96	2.73	0.00/0.00	0.41
Pd	4ND	2.02	6.78	0.00/0.00	0.45
	3NV	2.18	4.23	0.00/0.00	0.37
Pt	4ND	2.02	8.37	0.00/0.00	0.26
	3NV	2.00	4.53	0.00/0.00	0.26
Au	4ND	2.10	4.10	0.27/1.00	0.42
	3NV	2.41	2.80	0.33/1.00	0.19

[a] The average TM–N bond length

TMs, including Pd, Pt, and Au, scalar relativistic effect (DSPP) [41, 42] was considered when dealing with their core electrons. Spin-unrestricted DFT calculations were carried out in a periodically repeating tetragonal supercell with lattice constants of $a = b = 30$ Å and $c = 12.68$ Å. The supercell was large enough to neglect the interaction between its adjacent images. The Brillouin zone of the supercell was sampled by $1 \times 1 \times 5$ k points within the Monkhorst–pack scheme [47].

A (10, 0) single-wall CNT with the diameter of 7.93 Å was chosen in the present work. Two kinds of CN_x nanotube were considered, including 3NV and 4ND structures as shown in Fig. 1. The binding energy (E_b) of an individual TM on the CN_x nanotube was defined as: $E_b = E_{total}$ (CN_x nanotube) + E_{total} (TM) − E_{total} (TM/CN_x nanotube), where E_{total} denotes the total energy of the optimized system in the bracket. $E_b > 0$ corresponds a stable optimized configuration and indicates bonding.

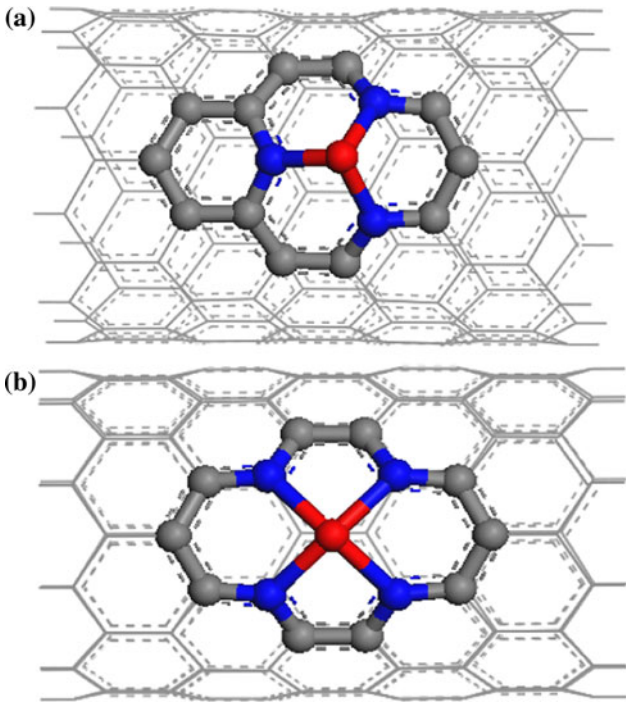

Fig. 2 The initial adsorption configurations of the TM on the **a** 3NV—and **b** 4ND–CN_x nanotube. *Gray*, *blue*, and *red* balls represent the carbon, nitrogen atoms, and TM, respectively

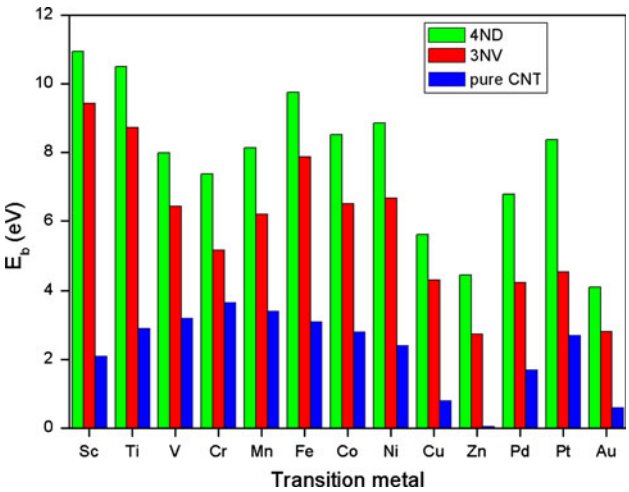

Fig. 3 The calculated binding energies (E_b) of 13 different TMs on the pure CNT and CN_x nanotubes with 3NV and 4ND defects

3 Results and discussion

3.1 TM adsorption on (10, 0) CN_x nanotube with 3NV or 4ND defect

First, we evaluate the stability of (10, 0) CN_x nanotubes with 3NV and 4ND defects by calculating their formation energies (E_f). Here, the formation energy is defined as

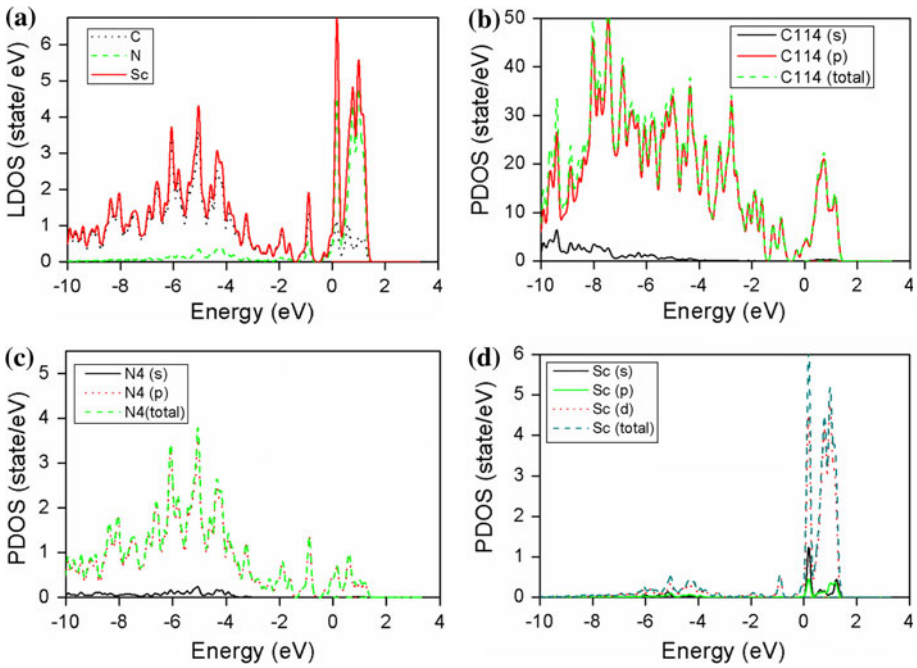

Fig. 4 **a** The local densities of states (LDOS) of a Sc adsorbed on the (10, 0) CN_x nanotube with 4ND defect ($C_{114}N_4$). The partial densities of states (PDOS) of **b** C, **c** N and **d** Sc in the adsorption system

$E_f = E_{tot} - n_C\mu_C - n_N\mu_N$, where E_{tot} is the total energy of the (10, 0) CN_x nanotubes, n_C, and n_N are the number of C and N atoms, respectively, and μ is the chemical potential. μ_C is obtained from the corresponding pure CNT, and μ_N is obtained from nitrogen in gas phase. The calculated formation energies of (10, 0) CN_x nanotubes with 3NV and 4ND defects are 3.05 and 2.87 eV, respectively, which are in good agreement with recent report [20]. We should point out that the formation energies of the two CN_x nanotubes are larger than that of graphite-like nitrogen (GN)-doped CNT, indicating that the GN nanotubes might be the most common in practical CN_x nanotubes.

When an individual TM atom is adsorbed on the CN_x nanotube, we consider two kinds of initial configurations: (1) the TM is directly bound to the site of 3NV or 4ND defect; (2) the TM is attached to the sites near 3NV or 4ND defect. After full structural optimization, we find that the TM adsorptions on the defect sites are the most stable because of their higher reactivity than other sites [15, 19, 20, 35–40]. Accordingly, in Table 1, we list the structural parameters and the corresponding binding energies of these most stable configurations of TMs on the two CN_x nanotubes (labeled as TM/CN_x nanotubes).

We find that these most stable configurations of TM/CN_x nanotubes are characterized as forming multiple TM–N bonds at the vacancy sites (Fig. 2) due to the N participation. All the TMs are projecting from the sidewall of the two CN_x nanotubes in various ways. Comparatively, the adsorbed TMs on the 3NV defect are more projecting than that of 4ND defect. Moreover, as shown in Table 1, the average TM–N distances (d_{TM-N}) of TM/CN_x nanotubes with 3NV and 4ND defects range from 1.83 (Fe) to 2.41 Å (Au) and from 1.92 (Ni) to 2.15 (Sc) Å, respectively.

On the other hand, due to the N participation and the vacancy defect, the binding energies of all TMs on the two CN_x nanotubes are generally larger than those on the pure CNT [48, 49] as shown in Fig. 3. Especially, the 4ND defect is more effective for enhancing the binding strength of the TM with nanotube than the 3NV defect. For instance, the binding energies for Ti, Zn, Pd, and Pt on CN_x nanotube with 4ND defect are 10.50, 4.44, 6.78, and 8.37 eV, respectively, while the binding energies are 8.72, 2.73, 4.23, and 4.53 eV, respectively, upon adsorption of Ti, Zn, Pd, and Pt on the CN_x nanotube with 3NV defect. Moreover, the variation of the binding energy as the number of d electrons (N_d) for these TMs is also given in Fig. 3. We find that Sc ($3d^14s^2$), Ti ($3d^24s^2$), and Fe ($3d^64s^2$) form the stronger bonds with E_b around 8 eV with respect to the others, which well agrees with previous study [37]. On the contrary, the binding energies of Zn ($3d^{10}4s^2$) on the two CN_x nanotubes are the smallest.

It is worthy of note that the binding energies of all TMs on the two CN_x nanotube exceed the cohesive energies of bulk TMs [50]. This indicates that these TMs might be atomic dispersion in the two CN_x nanotubes. To gain deep insight into this issue, we take Ti adsorption as an instance to calculate the diffusion of Ti from the vacancy site to its neighboring hexagon site. It is found that the Ti diffusion from the vacancy site to its neighboring hexagon-site on

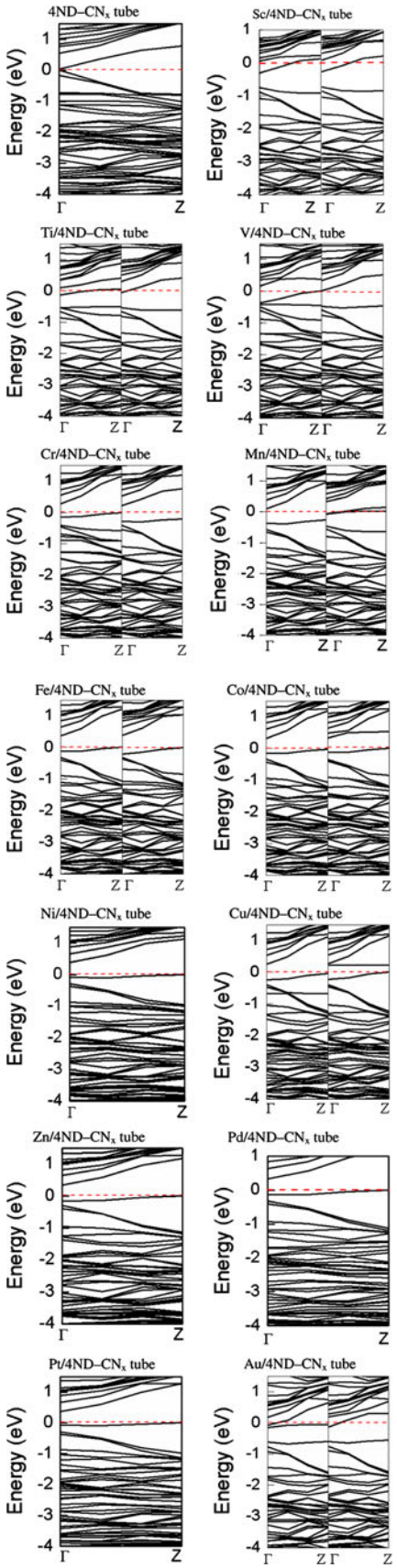

◀ **Fig. 5** The band structures of TM-adsorbed CN_x nanotube with 4ND defect. The Fermi level is set as zero and plotted with *red dotted line*. The *left* and *right* plots denote spin-up and spin-down band structures, respectively. Only one part indicates that this system is non-magnetic

the 3NV and 4ND defects is endothermic by 4.38 and 6.63 eV, respectively. Moreover, the energy barriers of Ti diffusion on the two CN_x nanotubes are as high as 6.92 and 7.46 eV, respectively. The endothermicity and larger barrier of Ti diffusion from the defect site to its neighboring site indicate that these Ti can be dispersed on each vacancy defect if a lot of vacancy defects exist in the CN_x nanotube. This phenomenon of the homogeneous dispersion of TM on defective nanotube has been previously observed in experiment for the adsorption of Pt nanoparticles on CN_x nanotube [29].

The strong interactions between these TMs and the two CN_x nanotubes can be explained through the local densities of states (LDOS) and partial densities of states (PDOS), i.e., Sc adsorption on the CN_x nanotube with 4ND defect as shown in Fig. 4. It is found that the d electrons of Sc and the p electrons of C and N atoms mainly contribute to the electronic states near Fermi level. In other words, strong interaction exists between the d orbitals of Sc and the p orbitals of N atoms due to their hybridization with each other.

3.2 The effects of chemical functionalization of TMs on the electronic properties of CN_x nanotubes

Chemical functionalization of nanotubes with the TM has been shown to be effective to modify their electronic properties. In this section, we mainly elucidate the effects of TMs adsorptions on the electronic properties of the two CN_x nanotubes. In Figs. 5 and 6, we present the band structures of different TM/CN_x nanotubes.

It can be seen that the CN_x nanotube with 4ND defect is a semiconductor with a small band gap ($\sim$0.06 eV) (Fig. 5), while the CN_x nanotube with 3NV exhibits metallic nature (Fig. 6), which are in good agreement with Li's study [20]. Upon adsorption of these TMs on the two CN_x nanotubes, certain impurity states are introduced into their band structures, rendering that their electronic properties are changed to different degrees, which is strongly dependent on the adsorbed TMs. For example, Ti adsorption makes the two CN_x nanotubes possess metallic nature, while the two CN_x nanotubes are transformed into half-metal materials upon adsorption of V or Mn on their surfaces. Moreover, when Cr, Fe, Co, Cu, Zn, Pd, or Pt is adsorbed on the two CN_x nanotubes, their band gaps are increased to different degrees due to the lift of the conduction bands of the two CN_x nanotubes. Thus, the several nanocomposites are still semiconductors.

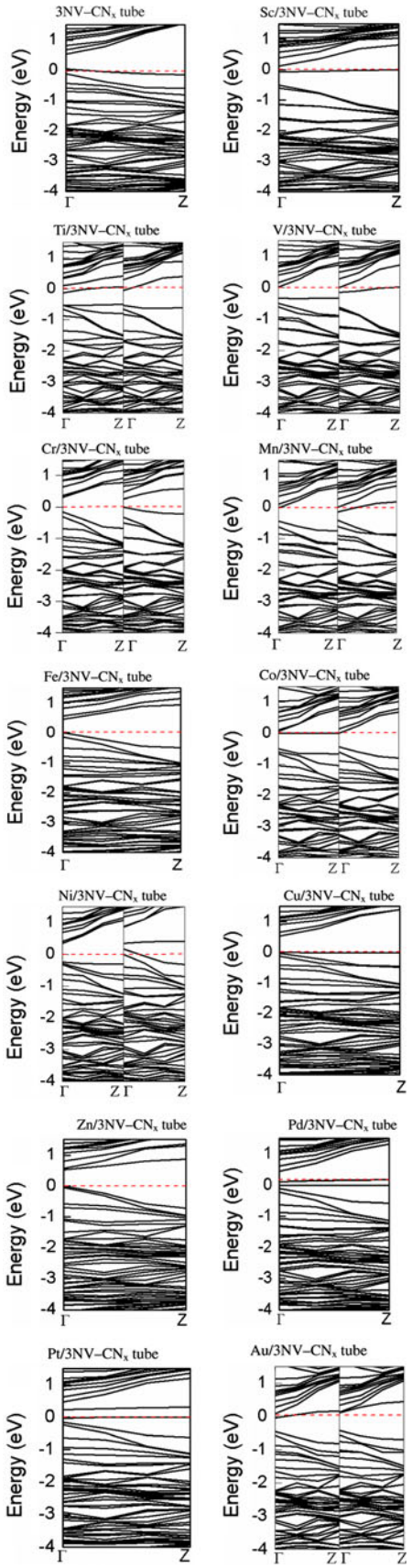

◀ **Fig. 6** The band structures of TM-adsorbed CN_x nanotube with 3NV defect. The Fermi level is set as zero and plotted with *red dotted line*. The *left* and *right* plots denote spin-up and spin-down band structures, respectively. Only one part indicates that this system is non-magnetic

Interestingly, three exceptions are Sc, Ni, and Au adsorptions, for which the influences on electronic properties of the two CN_x nanotubes are completely different: (1) for the Sc adsorption, the CN_x nanotube with 3NV defect is changed into a semiconductor with the band gap of 0.115 eV, while the CN_x nanotube with 4ND defect has metallic nature; (2) when Ni is adsorbed, the CN_x nanotube with 3NV defect is transformed into a half-metallic material, while the CN_x nanotube with 4ND defect is still a semiconductor, whose band gap is increased from 0.06 to 0.378 eV; (3) upon Au adsorption, the two CN_x nanotubes possess half-metallic (for 3NV defect) and metallic nature (for 4ND defect). This gives one an inspiration: CN_x nanotube-based devices with various electronic properties can be achieved.

The changes in band structures of the CN_x nanotubes upon adsorption of these TMs are also evident by the charge transfer between the TM and the CN_x nanotube. As shown in Table 1, in which we list the calculated charge transfer using Hirshfeld population analysis [51], the charges transferred from TMs to the CN_x nanotube with 3NV defect range from 0.70 e (for Sc) to 0.17 e (for Ni), while the range of charge transfer is from 0.65 e (for Sc) to 0.12 e (for Ni) in the case of 4ND defect CN_x nanotube. The charge transfer leads to the partially cationic of these TMs, and thus facilitating the adsorption of foreign species on these TM sites. On the other hand, we also evaluate the effects of TM adsorption on the magnetic properties of the two CN_x nanotubes. We find that the net magnetic moment emerges, ranging from 3.83 (for Cr/CN_x tube with 4ND defect) to 0 μ_B (for Zn/, Pd/ or Pt/CN_x nanotubes) as shown in Table 1. This is reasonable, because the ground states of the two CN_x nanotubes are non-magnetic, and the net spin magnetic moment mainly originates from the contributions of TMs.

4 Conclusions

In this paper, the chemical functionalization of pyridine-like and porphyrin-like CN_x nanotubes with 13 different TMs (Sc, Ti, V, Cr, Mn, Fe, Co, Ni, Cu, Zn, Pt, Pd, and Au) is systemically investigated using spin-polarized DFT calculations. We mainly focus on the effects of the chemical functionalization of TMs on the properties of the two CN_x nanotubes. The results indicate that the electronic and

magnetic properties of CN_x nanotubes can be effectively modified. For example, a CN_x nanotube with metallic nature can be obtained through the decoration of Ti, and the adsorption of V or Mn on the CN_x nanotube leads to the formation of a half-metallic nanomaterial, while we can obtain a semiconducting CN_x nanotube with different band gap by chemical functionalization with Cr, Fe, Cu, Zn, Pd, or Pt.

Acknowledgments This work is supported by the Committee of Education of Heilongjiang Province (11541095) and the Natural Science Foundation of Heilongjiang Province (ZD200820-01, B200814).

References

1. Tasis D, Tagmatarchis N, Bianco A, Prato M (2006) Chem Rev 106:1105
2. Zhao YL, Stoddart JF (2009) Acc Chem Res 42:1161
3. Khabashesku VN, Billups WE, Margrave JL (2002) Acc Chem Res 35:1087
4. Niyogi S, Hamon MA, Hu H, Zhao B, Bhowmik P, Sen R, Itkis ME, Haddon RC (2002) Acc Chem Res 35:1105
5. Banerjee S, Hermraj-Benny T, Wong SS (2005) Adv Mater 17:17
6. David AB, Khlobystov AN (2006) Chem Soc Rev 35:637
7. Gregory G, Wildgoose C, Banks E, Richard GC (2006) Small 2:182
8. Georgakilas V, Gournis D, Tzizios V, Pasquato L, Guldi DM, Prato M (2007) J Mater Chem 17:2679
9. White RJ, Luque R, Budairn VL, Clark JH, Macquarrie DJ (2009) Chem Soc Rev 38:481
10. Sen R, Satishkumar BC, Govindaraj A, Harikumar KR, Renganathan MK, Rao CNR (1997) J Mater Chem 12:2335
11. Terrones M, Terrones H, Grobert N, Hsu WK, Zhu YQ, Hare JP, Kroto HW, Walton DRM, Ph Kohler-Redlich, Rühle M, Zhang JP, Cheetham AK (1999) Appl Phys Lett 75:3932
12. Czerw R, Terrones M, Charlier JC, Blase XB, Foley R, Kamalakaran N, Grobert H, Terrones D, Tekleab PM, Ajayan W, Blau M, Carroll DL (2001) Nano Lett 1:457
13. Terrones M, Ajayan PM, Banhart F, Blase X, Carroll DL, Charlier JC, Czerw R, Foley B, Grobert N, Ph Kohler-Redlich, Rühle M, Seeger T, Terrones H (2002) Appl Phys A Mater Sci Process 74:355
14. Golberg D, Dorozhkin PS, Bando Y, Dong ZC, Tang CC, Uemura Y, Grobert N, Reyes-Reyes M, Terrones H, Terrones M (2003) Appl Phys A Mater Sci Process 76:499
15. Villalpando-Páez F, Romero AH, Mňoz-Sandoval E, Martínez LM, Terrones H, Terrones M (2004) Chem Phys Lett 386:137
16. Yu SS, Wen QB, Zheng WT, Jiang Q (2007) Nanotechnology 18:165702
17. Qiao L, Zheng WT, Xu H, Zhang L, Jiang Q (2007) J Chem Phys 126:164702
18. Min Y-S, Bae EJ, Kim UJ, Lee EH, Park NJ, Hwang CS, Park WJ (2008) Appl Phys Lett 93:043113
19. Rocha AR, Rossi M, Fazzio A, da Silva AJR (2008) Phys Rev Lett 100:176803
20. Li YF, Zhou Z, Wang LB (2008) J Chem Phys 129:104703
21. Gong KP, Du F, Xia ZX, Durstock M, Dai LM (2009) Science 323:760
22. Ayala P, Arenal R, Rümmeli M, Rubio A, Pichler T (2010) Carbon 48:575
23. Min YS, Bae EJ, Kim UJ, Lee EH, Park NJ, Hwang CS, Park WJ (2008) Appl Phys Lett 93:043113
24. Yoon H, Ko S, Jang J (2007) Chem Commun 14:1468
25. Shao Y, Sui J, Yin G, Gao Y (2008) Appl Catal B 78:89
26. Su FB, Tian ZQ, Poh CK, Wang Z, Lim SH, Liu ZL, Lin JY (2010) Chem Mater 27:832
27. Li XG, Park S, Popov BN (2010) J Power Source 195:445
28. Shao YY, Liu J, Wang Y, Lin YH (2009) J Mater Chem 19:46
29. Yue B, Ma YW, Tao HS, Yu LS, Jian GQ, Wang XZ, Wang XS, Lu YN, Hu Z (2008) J Mater Chem 18:1747
30. Jiang JS, Ma YW, Jian GQ, Tao HS, Wang XZ, Fan YN, Lu YN, Hu Z, Chen Y (2009) Adv Mater 21:4953
31. Zhou Y, Pasquareli R, Holme T, Berry J, Ginley D, O'Hayre R (2009) J Mater Chem 19:7830
32. Lepró X, Terrés E, Vega-Cantú Y, Rodríguez-Macías FJ, Muramatsu H, Kim YA, Hayahsi T, Endo M, Torres M, Terrones M (2008) Chem Phys Lett 463:124
33. Chen Z, Higgins D, Tao HS, Hsu RS, Chen ZW (2009) J Phys Chem C 113:21008
34. Sadek AZ, Zhang C, Hu Z, Partridge JG, McCulloch DG, Wlodarski W, Kalantar-zadeh K (2010) J Phys Chem C 114:238
35. Yang SH, Shin WH, Lee JW, Kim HS, Kang JK, Kim YK (2007) Appl Phys Lett 90:013103
36. Li YH, Hung TH, Chen CW (2009) Carbon 47:850
37. Feng H, Ma J, Hu Z (2010) J Mater Chem 20:1702
38. Titov AV, Zapol P, Král P, Liu DJ, Iddir H, Baishya K, Curtiss LA (2009) J Phys Chem C 113:21629
39. An W, Turner CH (2009) J Phys Chem C 113:7069
40. Stoyanov S, Titov AV, Krl P (2009) Coord Chem Rev 253:2852
41. Delley B (1990) J Chem Phys 92:508
42. Delley B (2000) J Chem Phys 113:7756
43. Wu XJ, Yang JL, Zeng XC (2006) J Chem Phys 125:044704
44. Wu XJ, Zeng XC (2006) J Chem Phys 125:044711
45. Zhao JX, Ding YH (2008) J Phys Chem C 112:2558
46. Perdew JP, Burke K, Ernzerhof M (1996) Phys Rev Let 77:3865
47. Monkhorst HJ, Pack JD (1976) Phys Rev B 13:5188
48. Durgun E, Dag S, Bagci V, Gulseren T, Yildirim CS (2003) Phys Rev B 67:201401
49. Durgun E, Dag S, Ciraci S, Gulseren O (2004) J Phys Chem B 108:575
50. Philipsen PHT, Baerends EJ (1996) Phys Rev B 54:5326
51. Hirshfeld FL (1997) Theor Chim Acta 44:129